JOURNAL OF THE KOREAN ASTRONOMICAL SOCIETY
39: 139 ~ 145, 2006

A STATISTICAL STUDY OF STREAMER-ASSOCIATED CORONAL MASS EJECTIONS

Y.-J. MOON[1], JIN-SUG KIM[1,2], Y.-H. KIM[1], K.-S. CHO[1], SU-CHAN BONG[1], AND Y. D. PARK[1],
[1] Korea Astronomy and Space Science Institute, Whaamdong, Yooseong-ku, Daejeon, 305-348, Korea
E-mail: yjmoon@kasi.re.kr
[2]Chungnam National University, Yooseong-ku, Daejeon, Korea
(Received October 2, 2006; Accepted October 23, 2006)

ABSTRACT

We have made a comprehensive statistical study on the coronal mass ejections (CMEs) associated with helmet streamers. A total number of 3810 CMEs observed by SOHO/LASCO coronagraph from 1996 to 2000 have been visually inspected. By comparing their LASCO images and running difference images, we picked out streamer-associated CMEs, which are classified into two sub-groups: Class-A events whose morphological shape seen in the LASCO running difference image is quite similar to that of the pre-existing streamer, and Class-B events whose ejections occurred in a part of the streamer. The former type of CME may be caused by the destabilization of the helmet streamer and the latter type of CME may be related to the eruption of a filament underlying the helmet streamer or narrow CMEs such as streamer puffs. We have examined the distributions of CME speed and acceleration for both classes as well as the correlation between their speed and acceleration. The major results from these investigations are as follows. First, about a quarter of all CMEs are streamer-associated CMEs. Second, their mean speed is 413 km s^{-1} for Class-A events and 371 km s^{-1} for Class-B events. And the fraction of the streamer-associated CMEs decreases with speed. Third, the speed-acceleration diagrams show that there are no correlations between two quantities for both classes and the accelerations are nearly symmetric with respect to zero acceleration line. Fourth, their mean angular width are about 60°, which is similar to that of normal CMEs. Fifth, the fraction of streamer-associated CMEs during the solar minimum is a little larger than that during the solar maximum. Our results show that the kinematic characteristics of streamer-associated CMEs, especially Class-A events, are quite similar to those of quiescent filament-associated CMEs.

Key words : Sun: coronal mass ejection—Sun: helmet streamer

I. INTRODUCTION

Coronal mass ejections (CMEs) are regarded as main causes of heliospheric and geomagnetic disturbances. A helmet streamer is a long lasting structure which is often associated with eruptive prominences (or filaments) and/or CMEs. There have been several studies (Sheeley et al. 1999; Andrews & Howard 2001; Moon et al. 2002) on the two classes of CMEs (flare-associated CMEs and filament-associated ones). Sheeley et al. (1999) suggested the following two distinct characteristics. First, there are gradual CMEs that are apparently formed when prominences and their cavities rise up from below coronal streamers. When seen broadside, their leading edges accelerate gradually to speeds in the range of $400 - 600\,\mathrm{km\,s^{-1}}$ before leaving 30 $R_\odot$. Second, there are impulsive CMEs, often associated with flares and Moreton waves on the visible disk. When seen broadside, these CMEs move uniformly across the $2 - 30\,R_\odot$ at speeds higher than $750\,\mathrm{km\,s^{-1}}$. At relatively large distances, impulsive events show clear evidence of deceleration. Andrews & Howard (2001) presented the height-time plots of several well-observed limb events, supporting the idea of the two CME classes. Moon et al. (2002) made a comprehensive statistical study of 3217 CMEs from 1996 to 2000 and found a significant statistical difference in the kinematics between the flare-associated and the filament-associated CMEs. In their study, they selected two classes according to temporal and spatial closeness between LASCO CMEs and their associated events (flares or quiescent filament eruption).

Even though filament-associated CMEs often occurred near helmet streamers, there have been only a few studies on the characteristics of streamer-associated CMEs. According to the SMM observation by Hundhausen (1993), about 50 % of the CMEs in 1984 result in streamer disruptions. Subramanian et al. (1999) classified 375 SOHO/LASCO CMEs (1996 January to 1998 June) into four types: (1) CMEs that disrupt the streamer (16%), (2) CMEs that have no effect on the streamer, even though they look related to it (46%), (3) CMEs that create streamer-like structures (8%), and (4) CMEs that are latitudinally displaced from the streamer (27%). They also argued that the second type CMEs should not interact with the streamers and the apparent associations may be due to the projection ef-

Corresponding Author: Y.-J. Moon

fect.

In the present study, we consider a total number of 3810 SOHO/LASCO CMEs from 1996 to 2000 and then use a rather restrictive criterion to select streamer-associated CMEs. This is the first attempt to statistically examine the kinematic characteristics of streamer-associated CMEs using such a large sample of events, which is about ten times of the number of events that Subramanian et al. (1999) examined. The criterion is that the CME initial eruption should occur in the pre-existing helmet streamer. It includes two cases: in the first, the CME morphology is quite similar to that of the pre-existing streamer and in the second the initial CME eruption occurred in a part of the streamer. Our selected events may be a subset of the first two types that Subramanian et al. (1999) classified. We expect that our restrictive criterion makes it possible to select a more homogeneous sample of events. Then we examine their kinematic characteristics and compare them with those of two classes of CMEs during the same period studied by Moon et al.(2002). In section 2, we explain our data. We present the results of our study with some discussion in section 3. A brief summary and conclusion are delivered in section 4.

II. DATA ANALYSIS

The Large Angle and Spectrometric Coronagraph Experiment (LASCO, Brueckner et al. 1995) C2 and C3 instruments are externally occulted white light coronagraphs that observe Thomson scattered visible light through broadband filters. The C2 instrument covers 2 to 6 solar radii with a pixel size of 12″, and the C3 instrument images 3.7-32 $R_\odot$ with a pixel size of 56 ″ . The height-time data of the CMEs used in this study are taken from the online SOHO/LASCO CME catalogue (http://cdaw.gsfc.nasa.gov/CME_list/), in which CME kinematics are estimated from LASCO C2 and C3 images. We have used a total number of 3810 CMEs from 1996 to 2000, which are all the CMEs identified by LASCO operators during the period. In the catalogue, CME speeds were determined from linear fits to the height-time measurements and accelerations were obtained from quadratic fits. Thus the speeds used in this study correspond to the representative speeds in the LASCO field of view. This task was independently performed by two authors of Yashiro et al. (2004) and the error was estimated at less than 10%. The acceleration measurements usually give a larger error than the speed measurements. The error in speed measurements gives a 20% maximum error in acceleration measurements according to the error propagation principle but this value may be larger when poor data are involved. To reduce the larger errors in the resulting accelerations, we only consider CMEs that have at least 5 data points. In addition, CMEs with vague leading edges were excluded since they may result in large errors in the resulting accelerations.

In this study, we adopted the following criteria to select the streamer-associated CMEs. First, we select CMEs whose morphological features are only seen in the helmet streamers. This criterion is purposed for minimizing ambiguity regarding the association between CMEs and streamers. Then we classify the selected events into two sub groups : Class-A events are CMEs whose morphological shape seen in the LASCO running difference image is quite similar to that of the pre-existing streamer seen in the corresponding LASCO image, and Class-B events are CMEs whose initial ejection occurred in a part of the streamer. Figure 1 shows a SOHO/LASCO CME that occurred on 1996 February 12. It is a typical Class-A event and its morphological shape looks similar to the helmet streamer seen in the LASCO image at 04:32. Such a type of CME may be caused by the destabilization of

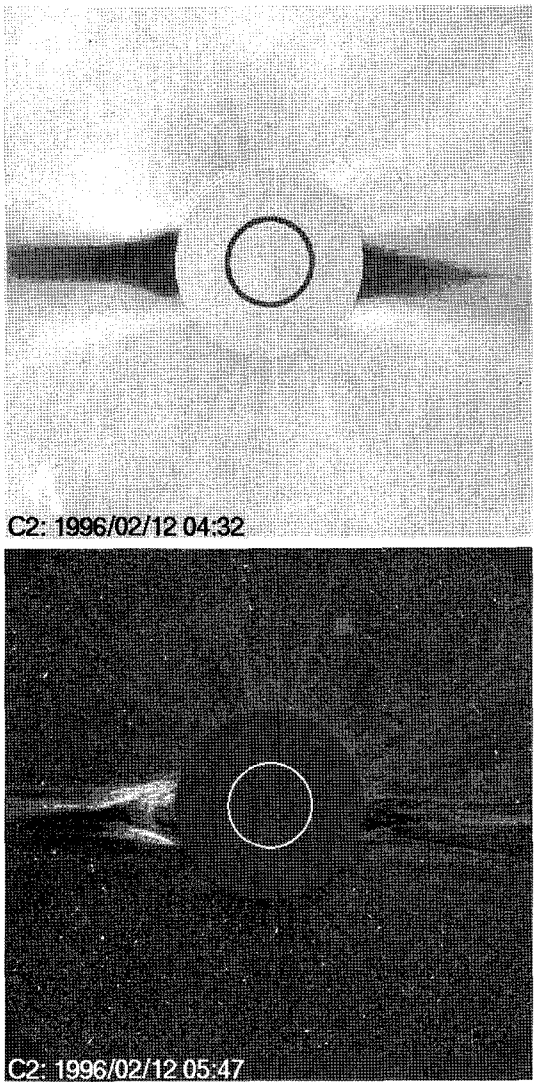

Fig. 1.— SOHO/LASCO C2 image (top) and its running difference image (bottom) for a Class-A streamer-associated CME (on the left limb) observed on 1996 February 12.

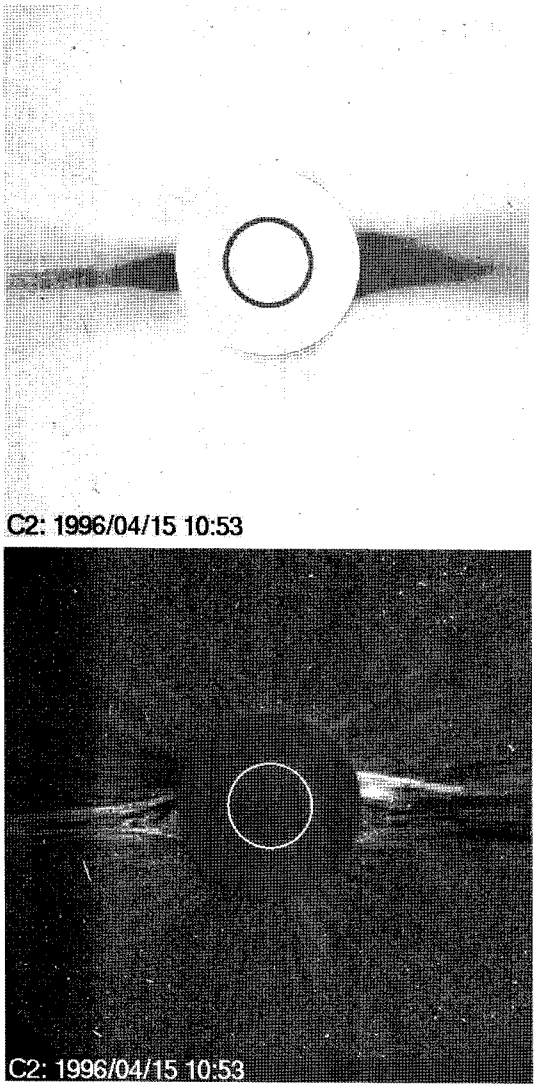

Fig. 2.— SOHO/LASCO C2 image (top) and its running difference image (bottom) for a Class-B streamer-associated CME (on the right limb) observed on 1996 April 15.

the helmet streamer (Wu & Guo 1997). Figure 2 shows a SOHO/LASCO CME that occurred on 1996 April 15. It is a typical Class-B CME that was ejected near the northern boundary of the helmet streamer. Such CMEs may be related to the eruption of a filament underlying the helmet streamer or narrow CMEs near the streamer. In the case of the narrow CMEs, they may be streamer puffs that move out along the streamer. According to Bemporad et al. (2005), the streamer puffs differ from streamer blowout CMEs in that (1) while the streamer is transiently inflated by the puff, it is not disrupted and (2) each puff comes from a compact explosion in the outskirts of the streamer arcade, not from an extensive eruption along the main neutral line of the streamer arcade. Using these above criteria, we have visually inspected SOHO/LASCO images of 3810

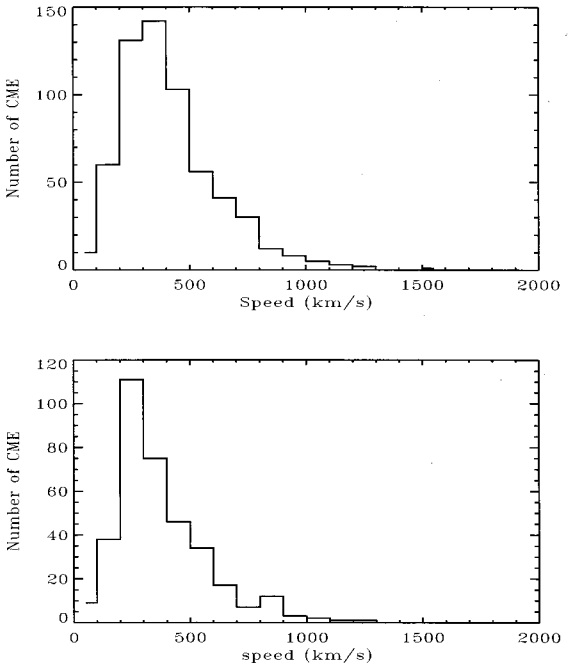

Fig. 3.— Speed histogram of streamer-associated CMEs: Class-A (top) and Class-B (bottom).

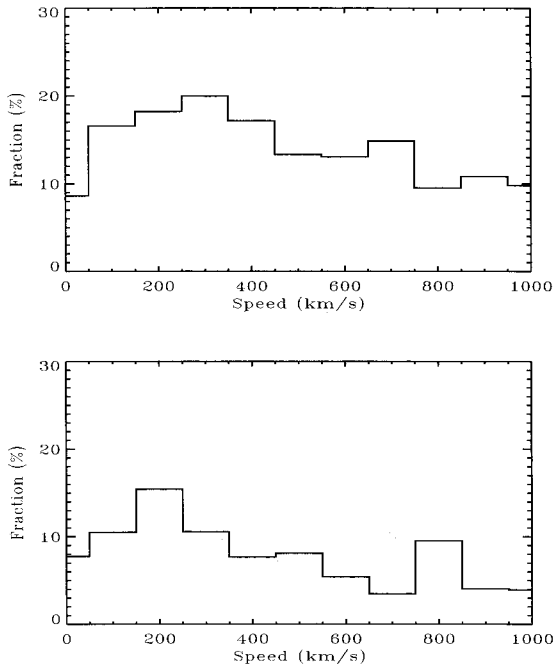

Fig. 4.— Fraction of streamer-associated CMEs relative to all the CMEs in each speed bin: Class-A (top) and Class-B (bottom).

CMEs and their running difference images.

III. RESULTS AND DISCUSSIONS

We have found a total of 960 streamer-associated CMEs, which corresponds to about a quarter of the total CMEs under consideration. This fraction is significantly lower than those of previous estimates (Hundhausen 1993; Subramanian et al. 1999). The reason is that we have used the restrictive criterion in order to obtain a more homogeneous sample of events. Note that our main interest is not to obtain the fraction of streamer-associated CMEs but to examine their kinematic characteristics.

Figure 3 shows speed histograms of two-classes of streamer-associated CMEs. Their mean speed is 413 km s^{-1} for Class-A events and 371 km s^{-1} for Class-B events, respectively. Comparing these values with the results of Moon et al.(2002) who examined two-classes of CMEs during the same period, we found that they are comparable to the mean speed (435 km s^{-1}) of the filament-associated CMEs but much smaller than those (534 km s^{-1} for > C1 class and 684 km s^{-1} for > M1 class) of the flare-associated CMEs. It is also noted that their major peaks in the histograms are located in the bin of 300-400 km s^{-1} for Class-A events and in the bin of 200-300 km s^{-1} for Class-B events. These results imply that most of the events correspond to slow CMEs. Figure 4 shows the fraction of the streamer-associated CMEs relative to all the CMEs in each speed bin for two class events. As seen in the figure, the fractions decrease with speed for both classes. This tendency is quite similar to that of filament-associated CMEs but quite different from that of flare-associated CMEs (Moon et al. 2002).

Figure 5 shows acceleration histograms for both classes. It is found that their mean accelerations are near zero for both cases. A careful inspection shows that the acceleration of Class-A events is a little skewed to positive acceleration with a mean value of about 2 m s^{-2}. The acceleration distribution is also quite similar to that of filament-associated ones (Moon et al. 2002). On the other hand, the acceleration histogram of Class-B events shows a nearly symmetric with respect to zero acceleration (constant speed). Figure 6 shows the speed-acceleration diagrams for streamer-associated CMEs. We found that there are no correlations between speed and acceleration for both cases and their distributions are nearly symmetric with respect to zero acceleration line (x axis). One noticeable difference between accelerating CMEs and decelerating ones is that the number of highly accelerating events is different from that of highly decelerating events. For Class-A events, while the number of CMEs whose acceleration is larger than 50 m s^{-2} is 10, that of CMEs whose acceleration is smaller than - 50 m s^{-2} is 4. For Class-B events, while the number of CMEs whose acceleration is large than 50 m s^{-2} is 3, that of CMEs whose acceleration is smaller than - 50 m s^{-2} is 6. Such a char-

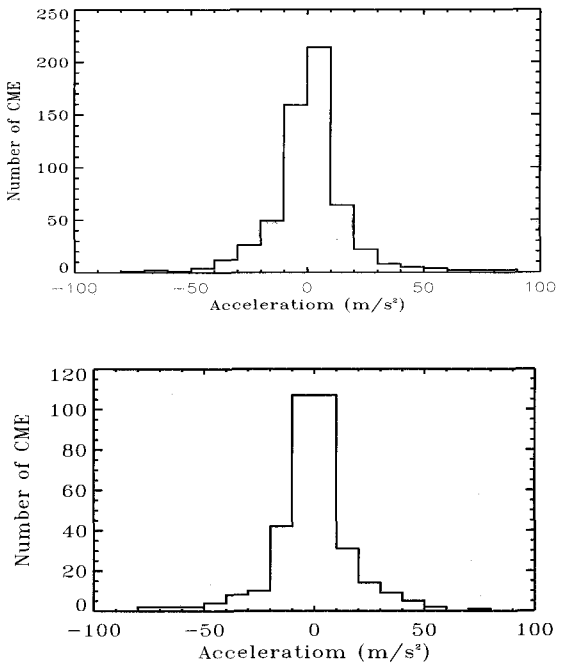

Fig. 5.— Acceleration histogram of streamer-associated CMEs: Class-A (top) and Class-B(bottom).

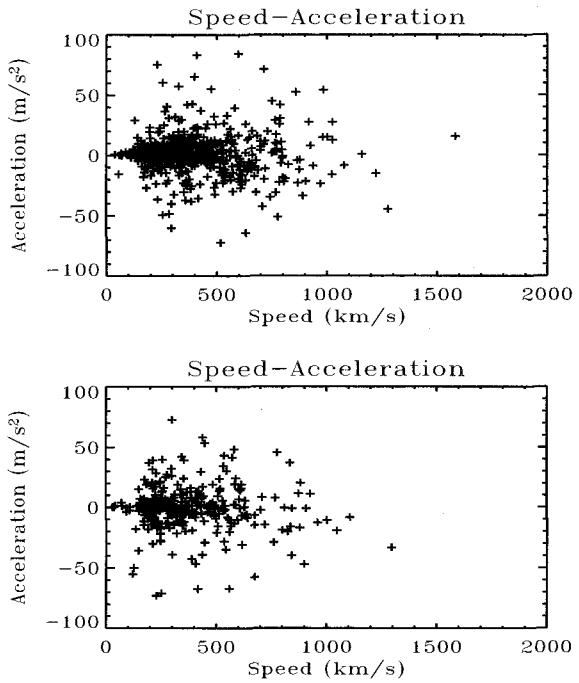

Fig. 6.— Speed-acceleration diagram of streamer-associated CMEs: Class-A (top) and Class-B (bottom).

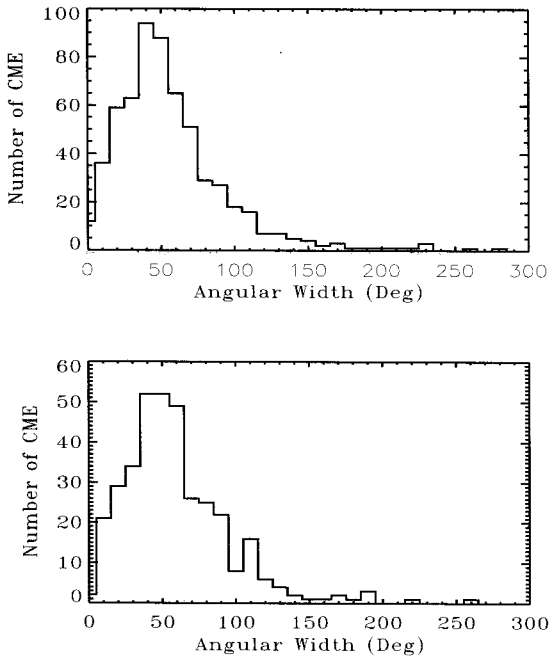

Fig. 7.— Angular width histogram of streamer-associated CMEs: Class-A (top) and Class-B (bottom).

acteristic for Class-A events is also similar to that of the filament-associated ones (Moon et al. 2002). But it is not clear that such differences are meaningful since the sample size is too small.

Figure 7 shows the histograms of angular width for streamer-associated CMEs. It is found that their major peaks are located near $40° \sim 50°$ for both classes and their mean angular widths are about 65 degrees. If we consider CMEs whose angular width are between 20° and 120° as Yashiro et al.(2004) did, their mean value is 57° for Class-A events and 61° for Class-B events, which are quite similar to that of normal CMEs (see Table 1 of Yashiro et al. 2004).

Figure 8 shows the solar cycle variation of the fraction of streamer-associated CMEs. As seen in the figure, the fraction during the solar minimum is a little larger than that during the solar maximum. This can be explained by the fact that CMEs are mostly detected around the equatorial region (near the helmet streamer) during solar minimum, while during solar maximum CMEs occurred at all latitudes where active regions are located (Yashiro et al. 2004).

IV. SUMMARY AND CONCLUSION

In this paper, we have made a comprehensive statistical study on the streamer-associated CMEs out of a total number of 3810 CMEs observed by SOHO/LASCO in 1996 to 2000. By comparing their LASCO images and running difference images, we picked out streamer-associated CMEs, which are classified into two subgroups: the Class-A events whose morphological shape seen in the LASCO running difference image is quite similar to that of the pre-existing streamer, and the Class-B events whose ejection occurred in a part of the streamer. As a result, we have found 960 streamer-associated CMEs. We have statistically examined several kinematic properties such as speed, acceleration, speed-acceleration correlation.

In Table 1, we summarize the kinematic statistics for several different CME association groups: streamer-associated, flare-associated, and filament-associated. The comparison among different groups shows that the kinematic characteristics of streamer-associated CMEs are similar to those of filament-associated ones but quite different from those of flare-associated ones. As shown in Table 1, the characteristics of Class-A events are more consistent with those of filament-associated ones. This may be understood by fact that Class-A events are more tightly associated with helmet streamers than Class-B events since the latter events may look being related to CMEs by the projection effect even though they are not linked to each other at all. There have been several studies on positive accelerations of streamer-associated events. Wu & Guo (1997) showed from numerical simulations that the speed of a CME caused by the destabilization of helmet streamer is continuously accelerated from 3 to 7 $R_\odot$. From SOHO/LASCO observations, Andrews & Howard (2001) presented good examples showing that CMEs associated with helmet streamers have constant accelerations, which are consistent with the characteristics of filament-associated CMEs. Moon et al. (2004) showed that a CME associated with the destabilization of a helmet streamer is accelerated from 2 to 11 $R_\odot$. Together with these studies, our results from the comprehensive statistical analysis show that the general kinematic characteristics of streamer-associated CMEs are similar to those of filament-associated ones.

To understand what makes the above similarity, it is important to determine the association between the streamer-associated CMEs and filaments. It is a time-consuming task to cross-check their association using all data in the present study. Thus we made a preliminary investigation using all the events in 1996. For 54 streamer-associated CMEs, we determined their association with filaments according to their temporal and spatial correlation using the NOAA NGDC (National Geophysical Data Center) filament activity data (http://www.ngdc.noaa.gov/stp/SOLAR/ftpfilaments.html #filaments). As a result, we found that a significant fraction (25/54) of the events were associated with filaments. Considering that about half of the CMEs come from behind the limb and the filament list is incomplete, we think that most of the streamer-associated CMEs are associated with filaments. This result hints that the mechanism of filament eruption and that of CME ejections in a streamer geometry have a certain common aspect though not identical. To draw a more

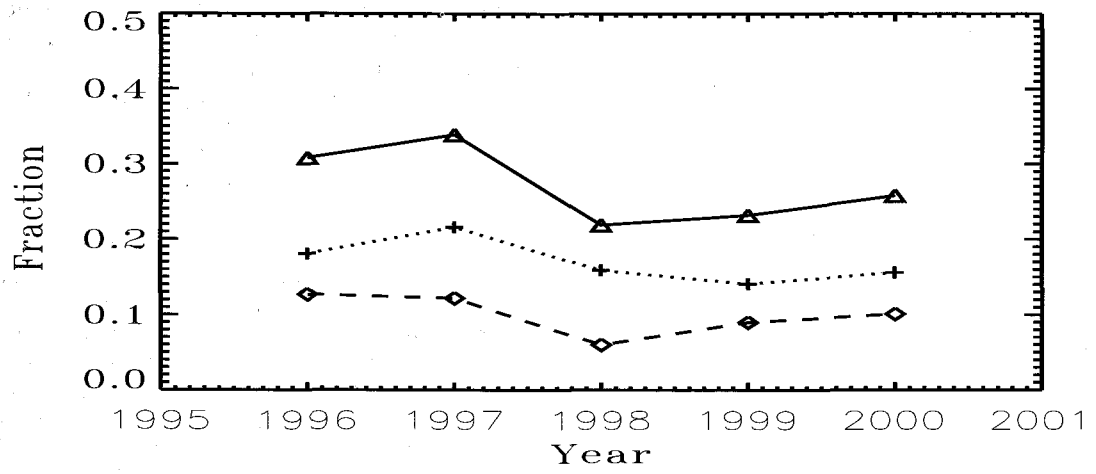

Fig. 8.— Solar cycle variation of the fraction of streamer-associated CMEs: The plus symbol is for Class-A, the diamond symbol is for Class-B, and the triangle symbol is for the whole sample.

TABLE 1.
SUMMARY OF KINEMATIC STATISTICS OF SOHO/LASCO CMES FOR DIFFERENT ASSOCIATION GROUPS FROM 1996 TO 2000

Associated Group	Speed(km/s)			Acceleration(m/s^2)			Reference
	Mean	Median	RMS	Mean	Median	RMS	
Streamer (A)	413	366	212	2	1	24	This Study
Streamer (B)	371	318	199	-1	0	26	This Study
Streamer (A+B)	397	349	208	1	1	24	This Study
All CMEs	477	420	269	-1	0	32	Moon et al.(2002)
Flare ($> C1$)	534	466	287	-2	-4	26	Moon et al.(2002)
Flare ($> M1$)	684	636	364	-5	-8	25	Moon et al.(2002)
Filament	435	359	255	3	1	19	Moon et al.(2002)

definite conclusion, it is necessary to investigate in more detail individual streamer-associated CMEs.

ACKNOWLEDGEMENTS

We really appreciate the referee's constructive comments. This work has been supported by the MOST grants (M1-0104-00-0059 and M1-0407-00-0001) and by the Korea Research Foundation (KRF-2005-070-C00059) of the Korean government. Jin-Sug Kim was supported by the Baekma Internship Program of Chungnam National University. The CME catalogue we have used is generated and maintained by the Center for Solar Physics and Space Weather, The Catholic University of America in cooperation with the Naval Research Laboratory and NASA. *SOHO* is a project of international cooperation between ESA and NASA.

REFERENCES

Andrews, M. D., & Howard, R. A., 2001, A Two-Type Classification of Lasco Coronal Mass Ejection, Space Science Review, 95, 147

Bemporad, A., Sterling, A. C., Moore, R. L., & Poletto, G., 2005, A New Variety of Coronal Mass Ejection: Streamer Puffs from Compact Ejective Flares, ApJ, 635, L189

Brueckner, G. E., et al., 1995, The Large Angle Spectroscopic Coronagraph (LASCO), Solar Phys., 62, 357

Hundhausen, A. J., 1993, Sizes and Locations of Coronal Mass Ejections - SMM Observations from 1980 and 1984-1989, J. Geophy. Res. 98, A10, 13177

Moon, Y.-J., Choe, G. S., Wang, H., Park, Y. D., Gopalswamy, N., Yang, G., & Yashiro, S., 2002, A

Statistical Study of Two Classes of Coronal Mass Ejections, ApJ, 581, 694

Moon, Y.-J., Cho, K. S., Smith, Z., Fry, C. D., Dryer, M. & Park, Y. D., 2004, Flare-Associated Coronal Mass Ejections with Large Accelerations, ApJ, 615, 1011

Sheeley, N. J., Jr., Watter, J. H., Wang, Y.-M., & Howard, R. A., 1999, Continuous Tracking of Coronal Outflows: Two Kinds of Coronal Mass Ejections, J. Geophy. Res. 104, 24739

Subramanian, P., Dere, K. P., Rich, N. B., & Howard, R. A., 1999, The Relationship of Coronal Mass Ejections to Streamers, J. Geophy. Res. 104, A10, 22321

Wu, S. T. & Guo, W. P., 1997, Numerical MHD Modeling of the Solar Driver for the Destabilization of a Coronal Helmet Streamer, Advances in Space Research, 20, Issue 12, 2313

Yashiro, S., Gopalswamy, N., Michalek, G., Rich, N., St.Cyr, C. O., Plunkett, S. P., & Howard, R. A., 2004, A Catalog of White Light Coronal Mass Ejections Observed by the SOHO Spacecraft, J. Geophy. Res. 109, A7, A07105